

## Research Article

# Modeling the Pathophysiology of Phonotraumatic Vocal Hyperfunction With a Triangular Glottal Model of the Vocal Folds

Gabriel E. Galindo,<sup>a</sup> Sean D. Peterson,<sup>b</sup> Byron D. Erath,<sup>c</sup> Christian Castro,<sup>a,d</sup>  
Robert E. Hillman,<sup>e,f,g</sup> and Matías Zañartu<sup>a</sup>

**Purpose:** Our goal was to test prevailing assumptions about the underlying biomechanical and aeroacoustic mechanisms associated with phonotraumatic lesions of the vocal folds using a numerical lumped-element model of voice production.

**Method:** A numerical model with a triangular glottis, posterior glottal opening, and arytenoid posturing is proposed. Normal voice is altered by introducing various prephonatory configurations. Potential compensatory mechanisms (increased subglottal pressure, muscle activation, and supraglottal constriction) are adjusted to restore an acoustic target output through a control loop that mimics a simplified version of auditory feedback.

**Results:** The degree of incomplete glottal closure in both the membranous and posterior portions of the folds

consistently leads to a reduction in sound pressure level, fundamental frequency, harmonic richness, and harmonics-to-noise ratio. The compensatory mechanisms lead to significantly increased vocal-fold collision forces, maximum flow-declination rate, and amplitude of unsteady flow, without significantly altering the acoustic output.

**Conclusion:** Modeling provided potentially important insights into the pathophysiology of phonotraumatic vocal hyperfunction by demonstrating that compensatory mechanisms can counteract deterioration in the voice acoustic signal due to incomplete glottal closure, but this also leads to high vocal-fold collision forces (reflected in aerodynamic measures), which significantly increases the risk of developing phonotrauma.

Vocal hyperfunction (VH) refers to (chronic) conditions of abuse and/or misuse of the vocal mechanism due to excessive and/or unbalanced (uncoordinated) muscular forces (Hillman, Holmberg, Perkell, Walsh, & Vaughan, 1989) and is associated with the most frequently occurring types of voice disorders (Bhattacharyya, 2014).

VH is believed to play a primary role in causing the chronic tissue trauma (referred to as phonotrauma) that leads to the formation of common vocal-fold lesions (e.g., vocal-fold nodules). Clinicians often describe this process as a vicious cycle (Hillman et al., 1989, 1990) in which the onset of tissue trauma interferes with vocal-fold closure and vibration, causing a progressive compensatory or reactive increase in hyperfunction (sometimes referred to as secondary VH) to maintain a desired level of phonation (on the basis of auditory feedback); this in turn leads to more tissue trauma and lesion formation.

<sup>a</sup>Department of Electronic Engineering, Universidad Técnica Federico Santa María, Valparaíso, Chile

<sup>b</sup>Mechanical and Mechatronics Engineering, University of Waterloo, Ontario, Canada

<sup>c</sup>Department of Mechanical & Aeronautical Engineering, Clarkson University, Potsdam, NY

<sup>d</sup>School of Speech and Hearing Sciences, Universidad de Valparaíso, Chile

<sup>e</sup>Center for Laryngeal Surgery & Voice Rehabilitation, Massachusetts General Hospital, Boston

<sup>f</sup>Harvard Medical School, Boston, MA

<sup>g</sup>MGH Institute of Health Professions, Boston, MA

Correspondence to Matías Zañartu: matias.zanartu@usm.cl

Editor: Julie Liss

Associate Editor: Jack Jiang

Received October 29, 2016

Revision received March 7, 2017

Accepted April 19, 2017

[https://doi.org/10.1044/2017\\_JSLHR-S-16-0412](https://doi.org/10.1044/2017_JSLHR-S-16-0412)

## Pathophysiology of VH

On the basis of clinical videoendoscopic observations of patients with hyperfunctional voice disorders, Morrison, Nichol, and Rammage (1986) postulated that a posterior glottal chink that extends into the membranous glottis can be a precursor to phonotrauma. Indirect support for this hypothesis was subsequently provided by Hsiung and Hsiao (2004), who observed a high prevalence of similar glottal configurations following surgical removal of phonotraumatic vocal-fold lesions and prior to vocal retraining (voice

**Disclosure:** The authors have declared that no competing interests existed at the time of publication.

therapy). Although the assumed potential causes of such abnormalities in glottal closure have not been definitively established (e.g., maladaptive response to emotional stress, reflux, excessive voice use with vocal fatigue), it is reasonable to assume that a posterior membranous chink would reduce vocal efficiency (the conversion of aerodynamic energy into acoustic sound energy) and could thus trigger the need to compensate (e.g., increase aerodynamic driving forces) to maintain the desired vocal output; this could, in turn, increase the potential for tissue trauma and initiate the vicious cycle of VH.

Although the role of the vicious cycle in the etiology of phonotraumatic vocal-fold lesions is widely accepted, the physical mechanisms that are assumed to underlie this phenomenon have not been verified because of the difficulties in obtaining *in vivo* measures of the relevant parameters. It is assumed that compensatory VH involves an increase in the contraction of intrinsic laryngeal muscles that adduct and stiffen the vocal folds (primarily the thyroarytenoid and lateral cricoarytenoid) in an effort to maintain closure of the membranous glottis and allow higher subglottal air pressure to develop in order to overcome the negative effects of tissue trauma on glottal closure and vocal-fold vibration. The resulting increase in aerodynamic driving forces is believed to be responsible for generating larger amplitudes of vocal-fold vibration and higher velocities of vocal-fold closure, which produce elevated vocal-fold contact pressures and collision forces that contribute to tissue trauma (Hillman et al., 1989, 1990). Sphincterlike constriction of the supraglottal structures of the larynx, sometimes referred to as *supraglottal compression* (Morrison & Rammage, 1993), is also often associated with compensatory VH, but its impact on, or role in, the pathophysiology of VH is not well understood, particularly because some studies have shown that such compression can sometimes also be observed in individuals with healthy voices (Behrman, Dahl, Abramson, & Schutte, 2003; Pemberton et al., 1993; Sama, Carding, Price, Kelly, & Wilson, 2001; Stager, Bielamowicz, Regnell, Gupta, & Barkmeier, 2000; Stager, Neubert, Miller, Regnell, & Bielamowicz, 2003). In addition, as observed in studies of vocal responses to the presence of noise (Grillo, Abbott, & Lee, 2010; Neils & Yairi, 1987; Stathopoulos et al., 2014), auditory feedback is pivotal in the regulation of laryngeal compensatory efforts and could thus play a key role in the etiology of VH. However, the role of auditory feedback in VH remains largely unexplored.

### ***Numerical Models Related to VH***

Numerical modeling offers the ability to gain insights into physical phenomena that cannot be directly observed. One such approach is the use of lumped-element models that can mimic and predict complex physical phenomena; they have been shown to be useful tools for the investigation of normal and pathological voice production (Erath et al., 2013; Kuo, 1998; Zhang, Tao, & Jiang, 2006). In terms of normal voice production, these models have also

been used to characterize the modal response of the vocal folds (Berry, Herzel, Titze, & Krischer, 1994), nonlinear fluid–tissue–sound interactions (Erath, Zaňartu, Peterson, & Plesniak, 2011; Titze, 2008; Zaňartu, Mongeau, & Wodicka, 2007), collision between vocal folds (Gunter, 2003; Horáček, Šidlof, & Švec, 2005; Ishizaka & Flanagan, 1972; Tao & Jiang, 2007; Tao, Jiang, & Zhang, 2006), asymmetric flow behavior (Erath & Plesniak, 2006; Pelorson, Hirschberg, Van Hassel, Wijnands, & Aurégan, 1994), and sound generation, propagation, and transmission through air and biological tissues (Story, 1995).

There have also been a few previous attempts to use numerical models to characterize pathological voice production. Samlan, Story, and Bunton (2013) used a kinematic model of voice production to explore how specific vocal-fold structural and vibratory features relate to breathy voice quality and the relation of perceived breathiness to some acoustic correlates of breathiness. Moisk and Esling (2014) used a lumped-mass model to determine that the vocal–ventricular fold coupling decreases pitch, increases vocal-fold damping, affects the vocal-fold mucosal wave, and reinforces irregular vibratory patterns. Dejonckere and Kob (2009) implemented a three-dimensional numerical model to test the theory that differences between male and female speakers in laryngeal structure and function contribute to the higher incidence of vocal nodules in female speakers. By mimicking and comparing glottal configurations and vocal-fold shapes for male and female speakers and manipulating subglottal air pressure and vocal-fold stress and tension, they were able to show that female versions of the model were more likely to produce an hourglass vibration pattern that would limit the collision zone between the vocal folds and facilitate “localized microtrauma” (i.e., the development of nodules).

Zaňartu et al. (2014), in the precursor to the present study, used modeling to focus on the potential role of compensation in phonotraumatic VH. VH was modeled by introducing a compensatory increase in lung air pressure to regain the vocal loudness level that was produced prior to introducing a large posterior opening of the cartilaginous (nonvibratory) glottis. This resulted in a significant increase in maximum flow-declination rate and amplitude of unsteady flow, thereby mimicking results from clinical studies (Hillman et al., 1989, 1990). In the current study, a low-order lumped-element model of the vocal folds was used to test prevailing assumptions about the physical mechanisms that underlie the role of compensatory VH in phonotraumatic voice disorders (i.e., the vicious cycle). The expanded modeling effort includes the addition of new factors representing zipperlike closure of the glottis during phonation, a posterior gap that can extend into the membranous (vibratory) glottis, simplified auditory feedback, selective activation of intrinsic laryngeal muscles, and supraglottal compression. The goal was to begin testing assumptions about the physical mechanisms that could contribute to the onset and perpetuation (vicious cycle) of phonotraumatic VH. This was accomplished by controlling the prephonatory positioning (posturing) of normal vocal folds

to create a posterior gap that extends into the membranous glottis to mimic the conditions that Morrison et al. (1986) proposed as preceding the onset of phonotrauma. This posturing was coupled with systematic adjustments in selected model parameters (levels of muscle activation, subglottal pressure, supraglottal compression) in an effort to approximate the previously achieved acoustic output, where complete glottal closure is present. This procedure mimics the efforts made (on the basis of auditory feedback) to compensate for the incomplete glottal closure. The proposed theory is that this type of modeling is capable of adequately representing the pathophysiologic mechanisms of interest so that key assumptions about these mechanisms can be effectively evaluated. Verification and/or better understanding of the pathophysiologic mechanisms associated with phonotraumatic voice disorders should contribute to improving the prevention and clinical management of these conditions.

## Method

The following section provides a description of the voice production model that was implemented. It also covers how the model parameters were adjusted to mimic phonatory compensation on the basis of the acoustic output of the model.

### Voice-Production Model

A numerical lumped-element model of the vocal folds with a triangular glottal shape is proposed, referred to as the triangular body-cover model (TBCM; see Appendix). The model is an extension of the body-cover model (BCM; Story & Titze, 1995), with the addition of a posterior glottal opening (Zañartu et al., 2014; see Figure A1) and the triangular glottal approach of Birkholz, Kröger, and Neuschaefer-Rube (2011a, 2011b; see the subsection Incomplete Glottal Closure in the Appendix). The numerical model consists of a series of masses interconnected with springs and dampers (represented as impedance boxes in Figure A1). The geometry of the masses is configured similarly to the anatomical structure of normal vocal folds. A detailed description of the model structure and behavior is presented in the Appendix.

One of the key features of the proposed TBCM is the representation of an incomplete glottal closure with a zipperlike closing shape, which produces a link between the posterior and membranous glottal openings (referred to as PGO and MGO, respectively). Incomplete closure is then controlled by the prephonatory positioning of the arytenoid cartilages and mimics the initial hyperfunctional configuration described by Morrison et al. (1986). We refer to this prephonatory positioning as a VH onset condition. The resulting membranous and posterior gaps were controlled by manipulating the prephonatory position and posturing of the arytenoid and fixing the muscular activation of the lateral and posterior cricoarytenoid muscles. The anatomical linkage between the PGO and MGO through the arytenoid rotation and displacement is a key feature of

the TBCM. Note that the arytenoid positioning yields a given posterior glottal distance (PGD), also known as *vocal-process distance*. In this article, we choose to represent incomplete glottal closure with PGD instead of the arytenoid positioning, for simplicity.

The arytenoids are pyramid-shaped cartilages that sit on top of the cricoid lamina (cricoarytenoid joints) and serve as the posterior points of attachment for the vocal-fold structures. They are manipulated by intrinsic laryngeal muscles that open and close the glottis (abduct and adduct the vocal folds). The thyroarytenoid (TA) muscle comprises the body of each vocal fold and contributes to changing the tension and length of the vocal folds, which can also simultaneously alter the position (rotation) of the arytenoids. Lateral cricoarytenoid muscles also contribute to changing the position of the arytenoids, primarily by approximating the arytenoids to close the glottis. Lastly, a set of interarytenoid muscles (transverse and oblique arytenoid muscles) control the proximity of the vocal process (Titze & Hunter, 2007).

For simplicity, the arytenoids were considered independent of the BCM control rules (Titze & Story, 2002), meaning that their rotation and displacement (and thus PGD) were not tied to muscle activation. This approach, although a simplification, allowed for convergence of the TBCM to the BCM without discarding the activation rules. The fact that arytenoid posturing is considered separately from the muscle-activation rules (Titze & Story, 2002) implies that the TBCM parameters (e.g., stiffness, damping, mass distribution) are obtained exactly as in the BCM, and the arytenoid motion is controlled separately. The fully controlled implementation of the arytenoid movement with extended physiological rules of muscle activation for the TBCM will be left for future studies.

To properly account for the physics of air leakage, a turbulent-flow component was added (Titze & Alipour, 2006). The area where turbulent flow was calculated corresponds to the total glottal area; therefore, the flow noise source  $U_n$  was modeled as

$$U_n = \begin{cases} N_f(\text{Re}^2 - \text{Re}_c^2) & \text{Re} > \text{Re}_c \\ 0 & \text{Re} \leq \text{Re}_c \end{cases}, \quad (1)$$

where  $N_f$  is a uniformly distributed random noise bounded by  $\pm 2 \times 10^{-6}$  L/s, which is filtered between 0.3 and 3 kHz with a second-order bandpass Butterworth filter;  $\text{Re}_c$  is a threshold number where the noise source is activated ( $\text{Re}_c = 1,200$ ); and  $\text{Re}$  is the Reynolds number, calculated by

$$\text{Re} = U_g \frac{D_H \rho}{A_g \mu}, \quad (2)$$

where  $U_g$  is the total volumetric glottal flow (membranous area + PGO),  $\rho$  is the air density,  $\mu$  is the dynamic viscosity of air, and  $D_H$  is the hydraulic diameter of the minimum glottal area  $A_g$ .

The default model parameters used in this study were obtained through an optimization process that is meant to mimic a simplified auditory-feedback mechanism. The target output was defined as the best objective representation of voice quality for a normal male voice. The configuration parameters obtained are shown in Table 1. The constriction of the supraglottal tract  $A_c^c$  was left unaltered at a value of 1, and the supraglottal pressure  $P_i$  was assumed to be 0. In this study, all simulations were performed using a truncated Taylor-series approximation (Galindo, 2017) to solve the governing differential equations. The default displacement of the arytenoids was set to  $a_r^d = 0$  (normal voice). A wave-reflection analog algorithm was used (Liljencrants, 1985) to propagate the acoustic pressure produced at the glottis with Level 2 interaction (Titze, 2008). The geometry of the vocal tract was set for a sustained /e/ vowel in a male speaker (Takemoto, Honda, Masaki, Shimada, & Fujimoto, 2006). The anatomical measures of the cartilages were obtained from Kim, Hunter, and Titze (2004). The arytenoid face  $L_a$  was considered to be 1.751 cm, with a 20% portion open to the flow channel (Hirano, Kurita, & Nakashima, 1981).

The measures used to quantify the characteristics of the determined voice configuration are a combination of the unsteady component of the glottal flow (AC-Flow), the maximum flow-declination rate (MFDR), the fundamental frequency ( $f_0$ ), the sound pressure level (SPL), the harmonics-to-noise ratio (HNR), and the signal-to-noise ratio. In addition, the net energy transferred (NET) to the vocal folds are measured, as defined by Thomson, Mongeau, and Frankel (2005), and the maximum contact pressure of the vocal folds (MCP), which is calculated as the maximum of the ratio between the vocal-fold contact force and contact area.

### Modeling Compensation in VH

An optimization framework, where we search for combinations of compensatory mechanisms that can reach a given acoustic target for various incomplete-closure scenarios, is proposed. Zañartu et al. (2014) did this by adjusting lung pressure to reach a target SPL. Here we extend this idea to include more control parameters and acoustic measures. Provided that acoustic measures of vocal function are used in the cost function, this optimization scheme can be viewed as mimicking a basic auditory-feedback loop. It is acknowledged that this approach is an oversimplification of the complex mechanisms involved in auditory feedback

**Table 1.** Default model parameters obtained through an optimization process.

Parameter	Expression	Value
Lateral cricothyroid muscle activation	$a_{LC}$	0.458
Thyroarytenoid muscle activation	$a_{TA}$	0.899
Cricothyroid muscle activation	$a_{CT}$	0.214
Arytenoid rotation	$a_r^d$	0.2°
Subglottal pressure	$P_s$	579 Pa

and does not account for psychoacoustic, sensorimotor, and cognitive components that play important roles in feedback control (Guenther, 1995). Nevertheless, the proposed optimization framework is a reasonable first approximation to represent a basic auditory-feedback mechanism in our self-sustained model of phonation.

To model hyperfunction, we create an onset-VH condition by fixing a prephonatory configuration that is created by rotating the arytenoids, thus affecting PGD. While maintaining a given PGD configuration, we explore the role of compensatory mechanisms to restore a target output. Three types of compensatory mechanisms are considered, on the basis of clinical and research observations: increased lung pressure, vocal-fold tension (increased muscle activation), and supraglottal compression (epilarynx tube narrowing; Sapienza & Stathopoulos, 1994; Sapienza, Stathopoulos, & Brown, 1997; Sperry, Hillman, & Perkell, 1994). We acknowledge that supraglottal compression may not play a role in compensation (to maintain an acoustic output) and might rather reflect simply a general increase in laryngeal muscle tension, particularly given the fact that it is also sometimes observed in subjects with normal voices (Behrman et al., 2003). Nevertheless, it is frequently associated with VH and was included in the study in an attempt to directly assess its potential contribution or role in compensation. We assume that the compensatory mechanisms do not change the initial posturing configuration, which remains fixed for each of the conditions under evaluation.

In terms of the target output, we aim to maintain voice quality, which is loosely defined as a selected group of objective measures of vocal function, for simplicity. Four acoustic measures are used to quantify the vocal output: SPL, harmonic richness factor (HRF),  $f_0$ , and HNR. All of these acoustic parameters consider the spectral components up to 5 kHz and are assumed to be sustained characteristics of phonation, meaning that neither intermittent cases nor variant cases are analyzed.

To represent the acoustic target in the optimization framework, a numerical space defined by

$$\delta(\omega) = \left( \sum_i^{\#\omega} \beta_i e^{|\omega_i/\tau_i|} \right) - 1 \quad (3)$$

is used to quantify a parametric distance, where  $\omega$  is a characteristic voice vector of cardinality  $\#\omega = 4$  with elements  $i \in \{\text{SPL}, f_0, \text{HRF}, \text{HNR}\}$ ;  $\beta$  is a vector of scaling factors related to the importance of each parameter in the cost function; and  $\tau$  is a dimensional tolerance factor used to regulate convexity across different parameters. In addition, a voice quality distance (QD) is defined as the parametric distance between a given voice vector  $\omega$  and a target characteristic voice vector  $\omega_T$ :

$$\text{QD}(\omega) = \delta(\omega - \omega_T). \quad (4)$$

This means that a given voice is closer to the desired target quality when the distance that separates them is shorter.

Given that the parametric distance function is composed solely of objective measures, the associated QD can be used as a cost function for the optimization process, seeking to minimize the distance between a voice vector  $\omega$  and the target voice vector. The parameter sets used for QD in this study are presented in Table 2. Note that other parameters, distance functions, and cost functions may yield different solutions. Thus, the results obtained in this study can only be guaranteed for the numerical space defined by Equation 3 and the parameters shown in Table 2. To ensure physiological relevance of the compensatory variables, subglottal pressure is bounded between 0 and 2,500 Pa, muscle activation must be in the range of [0, 1] (from no activation to full activation) for the TA and cricothyroid (CT) muscles, and supraglottal compression alters the epilarynx tube section  $A_e^c$  with a factor of 0.2–1.8, meaning it varies between 20% and 180% of the default area.

Arytenoid positioning can be measured in various ways, and it is often reported using the vocal-process distance and the glottal angle measured between glottal edges at the anterior commissure (see Appendix and Figure A2). For prephonatory conditions, the vocal-process distance (referred to as PGD in this article) has been reported to span up to 3 mm (Alipour, Scherer, & Finnegan, 1997; Berry et al., 2001; Regner et al., 2012; Scherer, Alipour, Finnegan, & Guo, 1997), and the glottal angle has been reported to span up to 10° (Cooke, Ludlow, Hallett, & Selbie, 1997; Dailey et al., 2005; Hunter, Titze, & Alipour, 2004; Stepp, Hillman, & Heaton, 2010). To match these ranges, we consider a positive rotation of the arytenoids  $a_r^o$  from 0° to 5°, in increments of approximately 0.08°, with no separation of its base ( $a_r^d = 0$ ), which leads to a glottal angle of up to 10° with a PGD of up to 3 mm. Note that maximum abduction arytenoid excursion can be much larger than the prephonatory values that we are considering in this study.

A Nelder–Mead optimization algorithm (Dennis & Schnabel, 1996) is used to find the minimum QD. This algorithm has shown good results in similar applications (Döllinger et al., 2002) and does not require a differentiable cost function to find local minima. The main disadvantage of this method is its inability to assure a global minimum; therefore, a random seeding approach is applied to minimize the error obtained in the prediction. For every compensated simulation, eight random seeds are taken with each parameter distributed uniformly over the valid range. Each seed is validated to ensure self-sustained oscillation. The best result is identified by the error value, which is obtained from the QD previously described.

In summary, the method used to model compensation is based on the modification of the arytenoid rotation, which yields increasing PGD and affects both the PGO and the MGO. This change alters both the dynamics of the system and the voice quality–related measures used in the cost function, thus increasing the QD, which is interpreted as nonoptimal quality. To restore (or minimize) QD, the control parameters (subglottal pressure, muscle activation, and supraglottal constriction) are conjointly modified according to the Nelder–Mead optimization algorithm.

## Results

Simulations and results are presented in three parts: model performance, parameter sensitivity, and impact of compensation. The model performance and validation are assessed by comparing the output of the new TBCM with that of the previously used BCM (Zañartu et al., 2014) and with actual human data. The parameter sensitivity shows the variation of the model output given the variation of each control parameter independently (subglottal pressure, muscle activation, supraglottal constriction, and arytenoid rotation). Compensation is assessed by varying the rotation of the arytenoids to produce incomplete glottal closure while adjusting model parameters to achieve a target acoustic output.

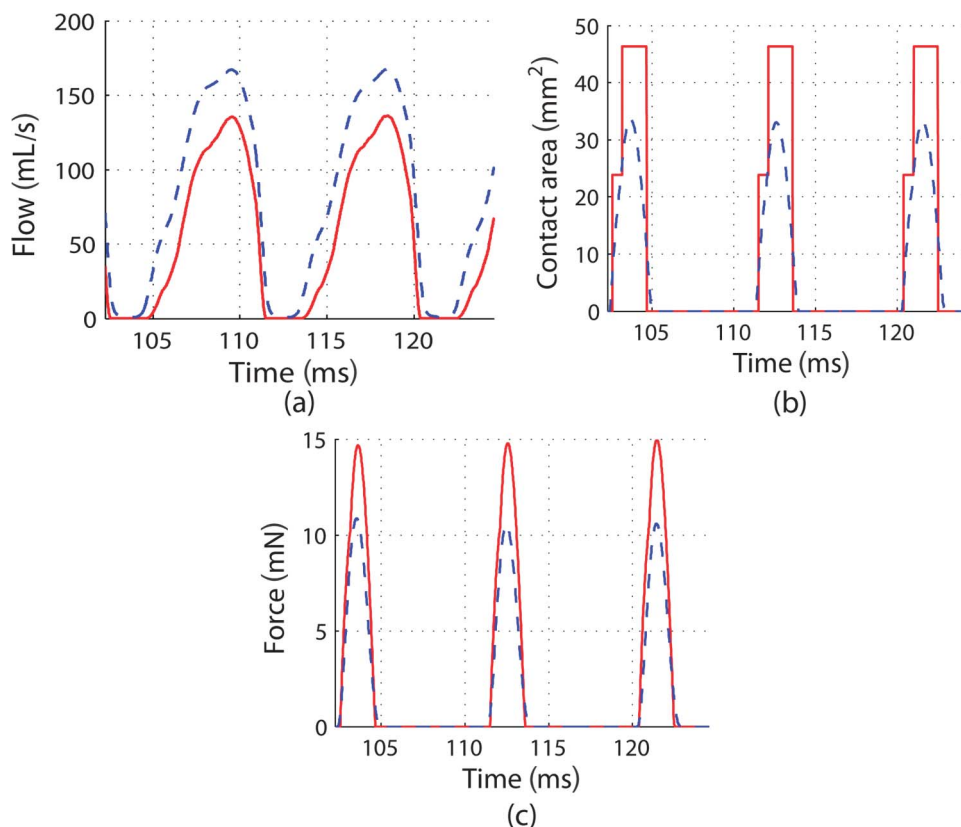
### Model Performance

Simulations were performed to contrast the behavior of the proposed TBCM and the previous BCM + PGO of Zañartu et al. (2014). A primary difference between these two models is the triangular glottis that is implemented in the TBCM, which configures vocal-fold contact differently and introduces a posterior gap that can extend into the membranous glottis. Both simulations used the same basic parameters to achieve the normal mean values for  $f_0$  and subglottal pressure ( $P_s$ ), which entailed using an arytenoid rotation of  $a_r^o = 0.5^\circ$  or its equivalent PGO of approximately 1 mm<sup>2</sup>. Outputs of glottal flow, contact force, contact area, and contact pressure were stored for each model (see Figure 1). These signals were synchronized with correlation techniques in order to compare their shapes and amplitudes. Some variations of vocal measures were observed ( $f_0$ , SPL, MFDR, minimum flow [Min-Flow], and the difference between maximum flow and Min-Flow [AC-Flow]), where the TBCM exhibits a 15% higher amplitude of the

**Table 2.** Proposed quality factors.

Measure	Expression	Scaling ( $\beta$ )	Target ( $\omega_T$ )	Tolerance ( $\tau$ )
Sound pressure level	SPL	0.4	81 dB	4 dB
Fundamental frequency	$f_0$	0.3	118 Hz	12 Hz
Harmonic richness factor	HRF	0.2	–10 dB	4 dB
Harmonics-to-noise ratio	HNR	0.1	43 dB	10 dB

**Figure 1.** Contrast between body-cover model (solid red line) and triangular body-cover model (dotted blue line) for (a) glottal air flow, (b) vocal-fold contact area, and (c) vocal-fold contact force due to the collision spring.



unsteady flow (AC-Flow), less rippling in the open phase, and a shorter closed portion.

Stronger differences can be observed in Figure 1b, in relation to the timing and amplitude of the vocal-fold contact area. For the BCM, the contact area is step shaped, which possibly distorts the vocal-fold pressure distribution and collision forces. Conversely, the TBCM produces a smoother contact area, resulting in a more realistic contact response when compared with electroglottographic signals (Titze, 1990). It is observed that the BCM contact force shows a similar shape to that of the TBCM in spite of the fact that the contact areas are considerably different. This is due to the self-oscillatory characteristics of the models, which produce similar power consumption on the closing phase even when they have different geometries.

An additional comparison was made to ensure that the model was in agreement with data from speakers with normal voices (Perkell, Hillman, & Holmberg, 1994). For this purpose, 100 simulations were run with parameters selected from random Gaussian distributions with mean values and standard deviations as shown in Table 3. Using these parametric variations, we aimed to contrast the model behavior with population-based studies, as in Robertson, Zañartu, and Cook (2016). The results from the simulations and a summary of human data from Perkell et al. (1994) are

presented in Table 4. There were no statistically significant differences ( $t$  test  $p < .005$ ) between the values generated by the TBCM and the data for the speakers with normal voices (TBCM-based values for SPL,  $f_0$ , MFDR, AC-Flow, Min-Flow, and  $P_s$  were all within 1  $SD$  of the normal mean values), thus supporting the use of the TBCM in the present study.

### Parameter Sensitivity

The parameter sensitivity provides a description of the effects of selected input parameters ( $P_s$ , PGD, cricothyroid muscle activation,  $A_c^c$ ) on the output of the model, on the basis of some of the vocal measures of interest (SPL,  $f_0$ , HNR). The input parameters are varied individually, and measures are compared using a normalized variation; this variation is a measure that scales each absolute value with the one obtained in the operational point (by default, 1 means no variation), thus allowing for direct comparisons of the various measure sensitivities. The actual ranges for the model parameters are shown in Table 5; the results of the parameter variation, in 64 steps, are presented in Figure 2. Only the parameter ranges where self-sustained oscillation was noted are reported.

**Table 3.** Operation point for model comparison.

Parameter	Expression (unit)	M (SD)	
		TBCM	BCM
Cricothyroid muscle activation	$a_{CT}$	0.202 (0.094)	0.222 (0.094)
Thyroarytenoid muscle activation	$a_{TA}$	0.834 (0.090)	0.867 (0.084)
Lateral cricothyroid muscle activation	$a_{LC}$	0.456 (0.000)	0.458 (0.000)
Supraglottal constriction	$A_e^c$	0.999 (0.190)	1.004 (0.195)
Subglottal pressure	$P_s$ (Pa)	577.3 (96.5)	578.2 (102.7)
Arytenoid rotation	$a_r$ (°)	0.2 (0.1)	0.5 (0.1)

Note. TBCM = triangular body-cover model; BCM = body-cover model.

Whereas PGD increased, SPL,  $f_0$ , and HNR decreased, reflecting what would be perceived as a softer, lower pitched, and breathier voice. Although better appreciated in our subsequent analysis, these parameters have a local maximum at a very small PGD, in agreement with previous studies that have argued that a small leak is beneficial in phonation (Zhang, 2015).

Increases in  $P_s$  produced an increase in SPL, which is consistent with previous work (Zañartu et al., 2014); an increase in  $f_0$ , which is well known in the literature (Titze & Alipour, 2006); and an increase in HNR, most likely due to the stronger driving pressure. The variation of muscular activations for the CT muscles produced diverse effects on spectral parameters ( $f_0$  and HNR). These results are consistent with the ideas that CT activation and TA activation have antagonistic effects on vocal-fold stress and strain (Chhetri, Neubauer, & Berry, 2012) and that the operational point, chosen by the optimization of the QD with data from Perkell et al. (1994), weights SPL more than HNR. Increasing the supraglottal constriction within the range of interest for this study (see Table 5) had only minor effects on all output measures.

To assess the contribution of each control parameter to the combined effect of the compensatory mechanism, a sensitivity analysis around the moving operational point was performed. The compensation algorithm was performed for different PGDs over the entire range of the study, and a series of operational points were obtained for each PGD. The variation of each parameter was set to 10% of its operational value. A normalization was

performed to scale the effects of different isolated compensatory mechanisms, such that the sum of all sensitivities for a given PGD is set to 1. Figure 3 illustrates the combined effect of all compensatory mechanisms across PGDs; we note that subglottal pressure is the most dominant input parameter for most PGDs, followed by CT muscle activation. As expected on the basis of their individual behavior, TA muscle activation and supraglottal compression had minor effects in the combined compensation effort.

### Assessing the Impact of Compensation

To assess the impact of compensation, the rotation of the arytenoids was varied from 0° to 5° in 64 steps in order to produce incomplete glottal closure (including both the cartilaginous and membranous glottis) that is measured in terms of the PGD. For each step, we fixed the glottal configuration and introduced compensatory mechanisms to restore a target output through the feedback process previously described. Selected measures of vocal function that have been linked to phonotraumatic VH (Hillman et al., 1989, 1990; Zañartu et al., 2014) were used to assess the effect of the compensatory action. Figure 4 shows the resulting MFDR, AC-Flow, MCP, and NET as functions of the PGD. Results are shown when compensation action is both present (compensated scenario) and absent (noncompensated). The higher variability of the compensated-scenario data may be explained by the optimization algorithm, which may become entrapped in local minima rather

**Table 4.** Clinical data for a normal male voice.

Measure	Expression (unit)	M (SD)		
		Perkell et al. (1994)	TBCM	BCM
Sound pressure level	SPL (dB)	77.8 (4.0)	74.9 (10.9)	77.9 (7.2)
Fundamental frequency	$f_0$ (Hz)	112.4 (11.8)	114.8 (18.8)	115.7 (22.2)
Maximum flow-declination rate	MFDR (L/s <sup>2</sup> )	337.2 (127.2)	281.8 (190.0)	308.8 (163.6)
Flow range	AC-Flow (L/s)	0.33 (0.07)	0.30 (0.17)	0.31 (0.15)
Minimum flow	Min-Flow (L/s)	0.08 (0.05)	0.08 (0.11)	0.05 (0.09)
Subglottal pressure	$P_s$ (Pa)	578.6 (107.9)	577.3 (96.5)	578.2 (102.7)

Note. TBCM = triangular body-cover model; BCM = body-cover model.

**Table 5.** Default and ranges for the input parameters in the triangular body-cover model.

Parameter	Expression (unit)	Default value	Range
Posterior glottal displacement	PGD (mm)	0.480	0–2.989
Subglottal pressure	$P_s$ (Pa)	900	0–2500
Cricothyroid muscle activation	$a_{CT}$	0.105	0–1
Thyroarytenoid muscle activation	$a_{TA}$	0.714	0–1
Supraglottal constriction	$A_e^c$	0.966	0.2–1.8

than the global minimum and thus produce outlier measures. Therefore, a trend line using a linear fit is also shown to facilitate the interpretation of the results of this case.

Figure 4a shows that when the gap becomes larger, AC-Flow becomes much smaller if no attempts to compensate are present. However, when we compensate for the reduction in QD (given by a combination of SPL,  $f_0$ , HRF, and HNR), the lack of closure and the compensatory action lead to a significantly increased AC-Flow and MFDR, both being more than doubled relative to normal for larger PGD. Higher-than-normal AC-Flow and MFDR are key features of patients with phonotraumatic VH and has been interpreted as reflecting the vicious cycle associated with these disorders (Hillman et al., 1989,

1990). Figure 4c shows that the impact on collision (MCP) as a function of PGD follows the same increasing trend as AC-Flow, MFDR, and NET; that is, a marked increase in collision forces was observed when compensation was applied to offset an increase in PGD. This behavior is again repeated for the energy transferred to the vocal folds as the PGD increases. In the noncompensated case, NET decreases with incomplete glottal closure, whereas in the compensated condition it shows a marked increase that is consistent with those observed for MCP, MFDR, and AC-Flow. In addition, it can be seen in the noncompensated cases of Figure 4 that AC-Flow, MFDR, and NET have a local maximum at a PGD of approximately 0.2 mm, which agrees with the idea that a small leak can improve efficiency in phonation (Zhang, 2015).

**Figure 2.** Effect of the model inputs on selected normalized vocal measures. Model inputs: (a) subglottal pressure, (b) posterior glottal displacement (PGD), (c) cricothyroid muscle activation, and (d) supraglottal constriction. Model outputs represented as: blue crosses: harmonics-to-noise ratio; red circles: sound pressure level; green asterisks: fundamental frequency.

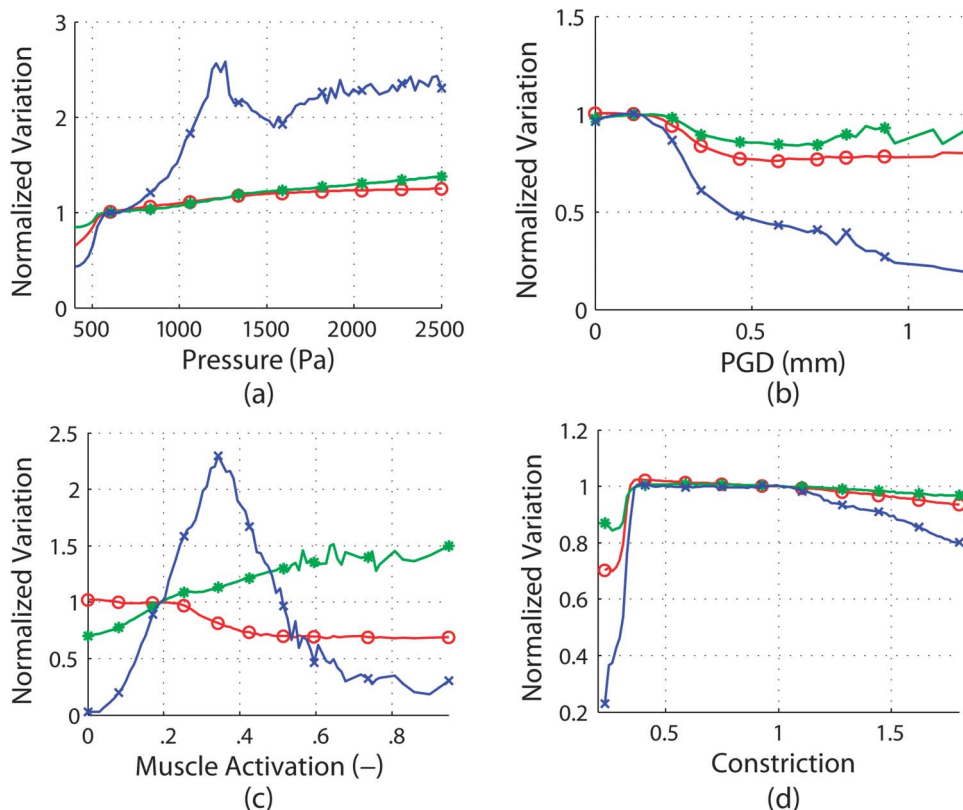


**Figure 3.** Combined effect of the compensatory mechanisms in terms of their normalized variation as a function of the posterior glottal displacement (PGD). Model inputs represented as: blue crosses: subglottal pressure; red circles: cricothyroid muscle activation; green asterisks: thyroarytenoid muscle activation; black diamonds: supraglottal constriction.

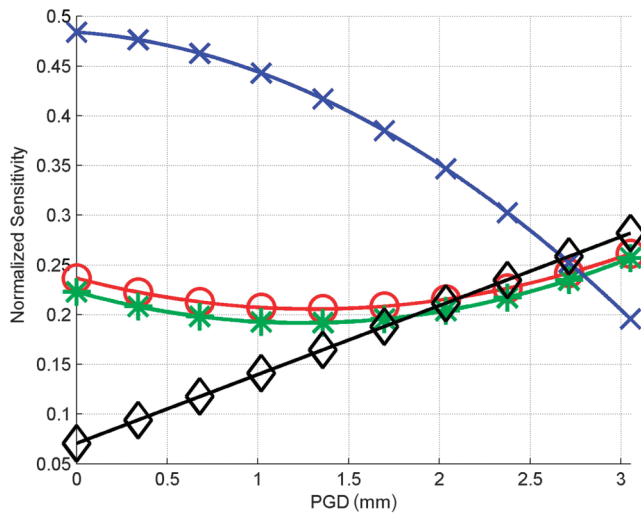
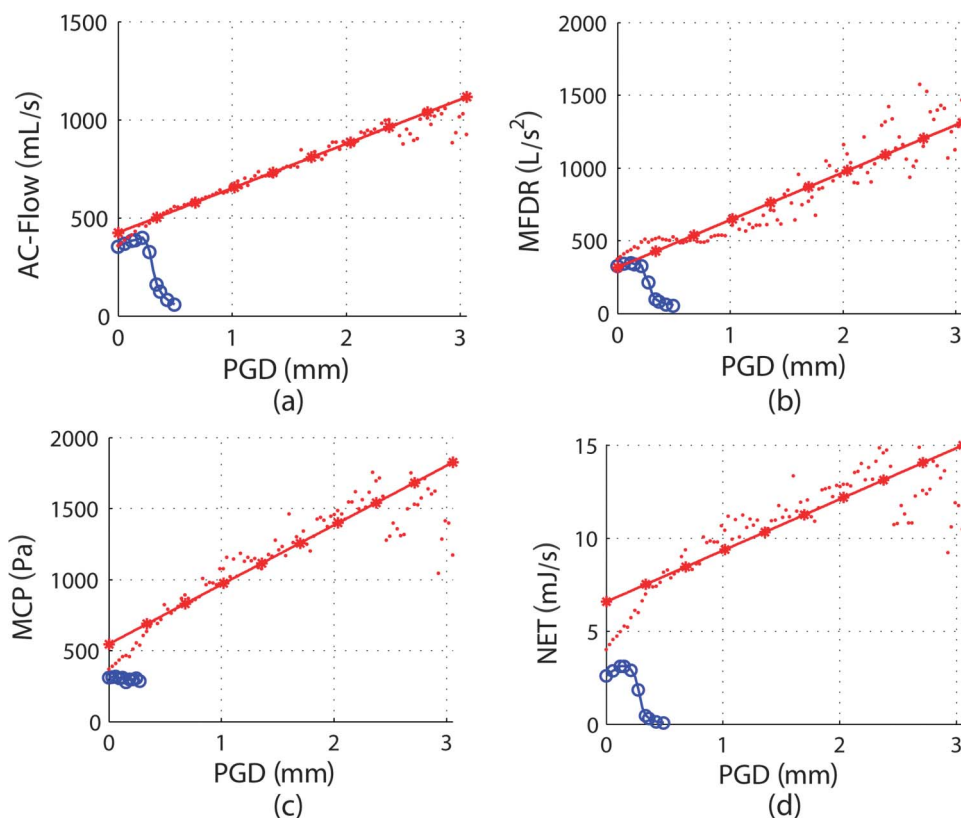
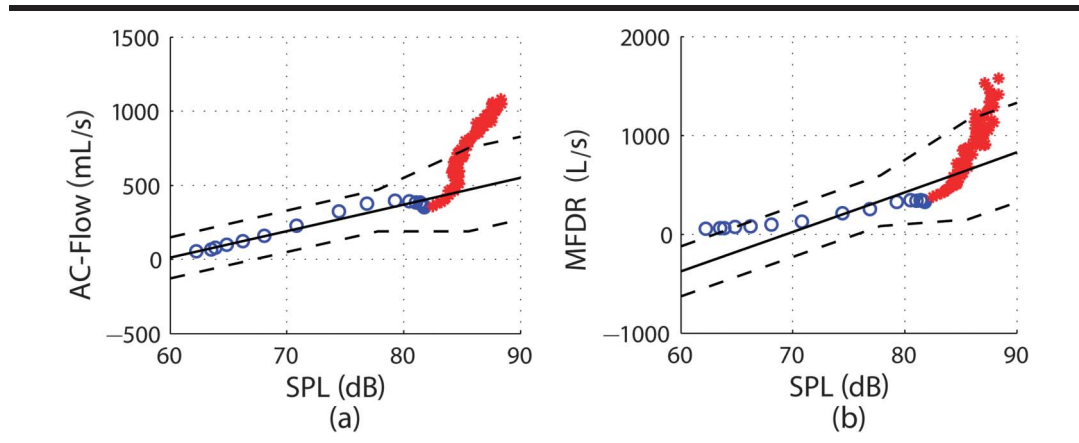


Figure 5 shows the impact of compensation on AC-Flow and MFDR as SPL is increased, on the basis of a regressed z-score analysis. This approach allows for comparing individual observations of aerodynamic parameters to normative sets of data (all measures converted to mean = 0 and  $SD = 1$ ) while at the same time adjusting or correcting the measures for the effects of SPL and  $f_0$  (on the basis of regression analyses of underlying correlations). This method has been used in previous work to identify measures for individual phonotraumatic patients with abnormal voices (exceeding 2  $SDs$ ) after adjusting or correcting for the impact on the measures of SPL (Hillman et al., 1989, 1990) and further applied in subsequent studies and applications (Llico et al., 2015; Zañartu et al., 2014). Using the same principles as Zañartu et al. (2014) and Llico et al. (2015), we linearly extended the normal bounds to provide a continuous function for the z-score assessment. The results in Figure 5b are based on the normative data from Perkell et al. (1994) and show that the AC-Flow values for the noncompensated condition are within normal limits, but that the values exceed the normal range in the compensated condition as PGD increases. These findings are consistent with previous results for patients with phonotrauma (Hillman et al., 1989, 1990).

**Figure 4.** Selected output measures under increasing incomplete glottal closure as a function of the posterior glottal displacement (PGD). (a) Flow range (AC-Flow), (b) Maximum flow-declination rate (MFDR), (c) maximum contact pressure (MCP), (d) net energy transfer (NET). Blue circles: noncompensated case; red asterisks: compensated case; solid red line: linear fit with  $R^2$  values of AC-Flow = .9808, MFDR = .8630, MCP = .8758, NET = .7226.



**Figure 5.** Regressed z score versus sound pressure level (SPL) for (a) flow range (AC-Flow) and (b) maximum flow-declination rate (MFDR). Blue circles: noncompensated case; red asterisks: compensated case; solid black line: z-score mean; dashed black line: z-score double standard deviation.



## Discussion

The formation of benign vocal-fold lesions (e.g., nodules) is believed to result from chronic detrimental patterns of vocal behavior, which we now refer to as phonotraumatic VH (Mehta et al., 2015). It is believed that a key component of these disorders is the vicious cycle that develops as patients attempt to maintain the loudness and quality of their voices following the onset of vocal-fold tissue trauma (Hillman et al., 1989, 1990). However, challenges associated with obtaining relevant *in vivo* measures have precluded the verification and quantification of these phenomena. We recently provided an initial demonstration that lumped-element numerical models have the potential to provide new quantitatively based insights into the underlying biomechanical and aeroacoustic mechanisms associated with the pathophysiology of these disorders, particularly with respect to the role of compensation (Zañartu et al., 2014). The present study extends our previous work by expanding the modeling framework to be more physiologically and clinically relevant, including better differentiation of glottal closure (cartilaginous versus membranous), the addition of other mechanisms that may play a role in compensation, and a first approximation of how auditory feedback might affect compensation.

In line with our previous efforts (Zañartu et al., 2014), we postulate that phonotraumatic VH is associated with biomechanical deficiencies that are exacerbated by abnormal compensations that can be quantitatively described through physics-based modeling. This study provides a numerical-modeling framework that attempts to mimic the underlying physical mechanisms associated with phonotraumatic VH. Rather than modeling vocal-fold lesions (e.g., Jiang, Diaz, & Hanson, 1998; Kuo, 1998), we start by modeling a normal voice and then alter it by introducing an incorrect glottal configuration and compensatory mechanisms to restore a target output through a feedback process. This scenario mimics the clinical descriptions from Morrison et al. (1986) and Hsiung and Hsiao (2004) proposing that a

posterior glottal opening that extends into the membranous glottis can be a precursor to phonotrauma. The approach extends the efforts of Dejonckere and Kob (2009) by expanding the analysis to include a closed-loop framework that can mimic the vicious cycle of VH with further compensatory mechanisms and a first approximation to auditory feedback, as well as focusing on the correlation between clinical measures of interest for the assessment of vocal function.

When varying the PGD (due to the arytenoid rotation), we noted that various measures of interest were significantly reduced in magnitude. In order of significance, this affected SPL, HRF, HNR, and  $f_0$ . We argue that this reduction for increasing PGD is a result of the strong non-linear source-filter interactions (Titze, 2008) that occur with increasing incomplete glottal closure due to the reduction of the source impedance. It can also be extracted from Figure 2 and Figure 4 (for the noncompensated scenario) that several parameters have a local maximum at a very small PGD, in agreement with previous studies arguing that a small leak is beneficial in phonation (Zhang, 2015). This feature is believed to be associated with the connection between the membranous and posterior gaps in the proposed voice-production model in this study, because it was not seen in our prior efforts (Zañartu, et. al 2014). Figures 2 and 3 also illustrate that the effect of increasing the posterior glottal gap can be counterbalanced, primarily, by increasing lung pressure and muscle activation. The finding that supraglottal constriction did not appear to play a significant role in compensation, combined with previous studies showing that it can sometimes also be observed in individuals with healthy voices (Behrman et al., 2003; Pemberton et al., 1993; Sama et al., 2001; Stager et al., 2000, 2003), casts some further doubt on the validity of using clinical (endoscopic) observations of supraglottal compression as a metric for assessing VH.

On the basis of the clinical observations and associated hypotheses of Hsiung and Hsiao (2004) and Morrison et al. (1986), we created a static or fixed posterior glottal

opening to mimic an onset or triggering condition for VH. A feedback mechanism was then implemented that attempted to reach a target for the four selected measures (SPL, HRF, HNR, and  $f_0$ ), using lung pressure, supraglottal constriction, and muscle activation as compensatory mechanisms. Maintaining these four measures within a given region is related to the idea of sustaining a desired loudness and quality—that is, to compensate for the voice becoming too soft, breathy, and/or outside of a typical pitch range. This approach constituted an optimization problem, where we searched for the optimal combination of compensatory mechanisms that maintain the selected acoustic measures within a desired range (with a given tolerance, as noted from Table 2) for various posterior glottal openings. The feedback mechanism can be related to an auditory control loop, although it does not capture the psychoacoustic and sensorimotor complexities of the auditory and neural systems. We realize that the compensatory mechanisms could also affect the glottal configuration that we have assumed remains fixed for simplicity. Nevertheless, we argue that the proposed approach is sufficiently valid for a first approximation or proof of concept, given evidence that patients with VH tend to maintain an incorrect glottal posturing (Hsiung & Hsiao, 2004; Morrison et al., 1986) prior to vocal retraining (voice therapy), and that signs of some of the proposed compensatory mechanisms have been observed in such patients (Hillman et al., 1989, 1990; Sapienza et al., 1997; Sapienza & Stathopoulos, 1994; Sperry et al., 1994).

When modeling phonotraumatic VH with the compensatory mechanisms in place, we observe that an increasing (membranous and posterior) gap due to incorrect posturing leads to increased AC-Flow, MFDR, and vocal-fold collision forces (see Figure 4). Increased AC-Flow and MFDR are key features of patients with VH and they have been associated, along with increased vocal-fold collision forces, with a vicious cycle in VH. Similar behavior is seen in the regressed  $z$ -score analysis that contrasts our simulations with human recordings (Hillman et al., 1989, 1990). It is important to highlight that the acoustic output remains the same (within the given tolerance).

Our results point to a high correlation between AC-Flow and MFDR with vocal-fold collision forces. These correlations are expected to be physiologically relevant but also possibly related to our modeling assumptions. We plan on further validating our numerical simulations with physical experiments using silicone models (Murray & Thomson, 2012) to better understand the relation between collision forces and aerodynamic measures. Note that a stronger determinant of impact force may be given by the maximum area declination (Titze, 2016). However, maximum area declination currently has less potential as a routine clinical measure than the aerodynamic measures used in this study because it requires calibrated laryngeal high-speed videoendoscopic imaging that is more difficult (and much more expensive) to implement in a clinical setting. Therefore, our findings support the use of aerodynamic measures for the clinical assessment of vocal function because of their potential to provide insights into critical underlying

pathophysiological mechanisms that may not be adequately reflected in acoustic measures due to the types of compensation illustrated in this study. More attention is being placed on these measures in clinical studies (Mehta & Hillman, 2007), and they are also gaining attention in ambulatory studies (Llico et al., 2015; Mehta et al., 2015; Zañartu, Ho, Mehta, Hillman, & Wodicka, 2013). The observation that aerodynamic measures are potentially more sensitive to changes in underlying pathophysiology than acoustic measures has been previously suggested on the basis of studying treatment-related (voice therapy) vocal-function changes in patients with vocal nodules (Holmberg, Doyle, Perckell, Hammarberg, & Hillman, 2003).

Further research is needed to explore the correlations between vocal measures of interest in other scenarios because the cases investigated in this study and the modeling assumptions are based on modal phonation in normal male voices. Extensions to other groups and conditions (Robertson et al., 2016), including voice production in adult women and children, are pending. We anticipate that some of the correlations may be less significant in women and children because the expected higher source-filter interactions in those cases could create more variability in the relationships between aerodynamic measures and contact forces (Story & Bunton, 2013). However, the application to adult female voices is of great interest due to the higher prevalence of hyperfunction-related voice disorders in women (Roy, Merrill, Gray, & Smith, 2005). In addition, the presence of vocal-fold lesions (e.g., nodules) is expected to further reduce glottal closure (increase the glottal gap) and thus increase the difficulties, forces, and tissue trauma associated with phonation (an exacerbation of the vicious cycle).

Future efforts will be devoted to expanding this modeling effort in three major areas: describing the effects of vocal-fold lesions (e.g., nodules, polyps) within the proposed framework for phonotraumatic VH; incorporating physiological rules to link a comprehensive muscle activation with vocal-fold posturing for the TBCM; and creating psychoacoustic and sensorimotor representations to account for feedback and feed-forward mechanisms in the VH framework. The addition of these components would also allow for extending the proposed framework to explore nonphonotraumatic VH (e.g., muscle-tension dysphonia).

## Conclusions

In this study, we illustrated that numerical models of voice production can provide important insights into the pathophysiology of phonotraumatic VH by providing estimates of parameters that are not readily accessible, thereby enabling the investigation of potential key relationships between vocal dysfunction and compensation. To be specific, modeling was used to show that compensating (increased lung pressure and laryngeal muscle activation) for what has been described as a VH-onset condition (posterior glottal gap extending into the membranous glottis) can restore the target acoustic vocal output (SPL,  $f_0$ , HNR, HRF) but leads to high vocal-fold collision forces (which

is reflected in aerodynamic measures), and thus significantly increases the risk of developing phonotrauma. The onset of phonotrauma is expected to further increase compensatory forces, thus eliciting the vicious cycle that has been associated with phonotraumatic voice disorders (e.g., vocal-fold nodules). The results also point to the potential clinical value of using aerodynamic measures to help detect VH, and they further suggest possible limitations and risks associated with relying solely on auditory perceptual or acoustic measures to make clinical decisions about vocal function (e.g., for voice assessment and during voice therapy) because these parameters may not reliably reflect underlying VH due to compensation.

## Acknowledgments

Gabriel E. Galindo acknowledges scholarships from the Comisión Nacional de Investigación Científica y Tecnológica and Universidad Técnica Federico Santa María. This work was supported by Comisión Nacional de Investigación Científica y Tecnológica Grants FONDECYT 1151077, BASAL FB0008, and MEC 80150034 (awarded to Matías Zañartu), Ontario Ministry of Research and Innovation Grant ER13-09-269 (awarded to Sean D. Peterson), and National Institute on Deafness and Other Communication Disorders Grants R331DC011588 and P50DC015446 (awarded to Robert E. Hillman). The content is solely the responsibility of the authors and does not necessarily represent the official views of the National Institutes of Health.

## References

- Alipour, F., Scherer, R. C., & Finnegan, E. (1997). Pressure-flow relationships during phonation as a function of adduction. *Journal of Voice*, *11*, 187–194.
- Behrman, A., Dahl, L. D., Abramson, A. L., & Schutte, H. K. (2003). Anterior–posterior and medial compression of the supraglottis: Signs of nonorganic dysphonia or normal postures. *Journal of Voice*, *17*, 403–410.
- Berry, D. A., Herzel, H., Titze, I. R., & Krischer, K. (1994). Interpretation of biomechanical simulations of normal and chaotic vocal fold oscillations with empirical eigenfunctions. *The Journal of the Acoustical Society of America*, *95*, 3595–3604.
- Berry, D. A., Verdolini, K., Montequin, D. W., Hess, M. M., Chan, R. W., & Titze, I. R. (2001). A quantitative output-cost ratio in voice production. *Journal of Speech, Language, and Hearing Research*, *44*, 29–37.
- Bhattacharyya, N. (2014). The prevalence of voice problems among adults in the United States. *The Laryngoscope*, *124*, 2359–2362.
- Birkholz, P., Kröger, B. J., & Neuschaefer-Rube, C. (2011a, March). *Articulatory synthesis of words in six voice qualities using a modified two-mass model of the vocal folds*. Paper presented at the First International Workshop on Performative Speech and Singing Synthesis, Vancouver, British Columbia, Canada.
- Birkholz, P., Kröger, B. J., & Neuschaefer-Rube, C. (2011b). Synthesis of breathy, normal, and pressed phonation using a two-mass model with a triangular glottis. In P. Cosi, R. De Mori, G. Di Fabbriozio, & R. Pieraccini (Eds.), *Interspeech 2011: 12th Annual Conference of the International Speech Communication Association* (pp. 2681–2684). Baixas, France: International Speech Communication Association.
- Chhetri, D. K., Neubauer, J., & Berry, D. A. (2012). Neuromuscular control of fundamental frequency and glottal posture at phonation onset. *The Journal of the Acoustical Society of America*, *131*, 1401–1412.
- Cooke, A., Ludlow, C. L., Hallett, N., & Selbie, W. S. (1997). Characteristics of vocal fold adduction related to voice onset. *Journal of Voice*, *11*, 12–22.
- Dailey, S. H., Kobler, J. B., Hillman, R. E., Tangrom, K., Thananart, E., Mauri, M., & Zeitels, S. M. (2005). Endoscopic measurement of vocal fold movement during adduction and abduction. *The Laryngoscope*, *115*, 178–183.
- Dejonckere, P. H., & Kob, M. (2009). Pathogenesis of vocal fold nodules: New insights from a modelling approach. *Folia Phoniatrica et Logopaedica*, *61*, 171–179.
- Dennis, J. E., Jr., & Schnabel, R. B. (1996). *Numerical methods for unconstrained optimization and nonlinear equations*. Philadelphia, PA: Society for Industrial and Applied Mathematics.
- Döllinger, M., Hoppe, U., Hettlich, F., Lohscheller, J., Schuberth, S., & Eysholdt, U. (2002). Vibration parameter extraction from endoscopic image series of the vocal folds. *IEEE Transactions on Biomedical Engineering*, *49*, 773–781.
- Erath, B. D., & Plesniak, M. W. (2006). The occurrence of the Coanda effect in pulsatile flow through static models of the human vocal folds. *The Journal of the Acoustical Society of America*, *120*, 1000–1011.
- Erath, B. D., Zañartu, M., Peterson, S. D., & Plesniak, M. W. (2011). Nonlinear vocal fold dynamics resulting from asymmetric fluid loading on a two-mass model of speech. *Chaos*, *21*, 033113.
- Erath, B. D., Zañartu, M., Stewart, K. C., Plesniak, M. W., Sommer, D. E., & Peterson, S. D. (2013). A review of lumped-element models of voiced speech. *Speech Communication*, *55*, 667–690.
- Galindo, G. (2017). *Bayesian estimation of a subject-specific model of voice production for the clinical assessment of vocal function* (Unpublished doctoral dissertation). Universidad Técnica Federico Santa María, Valparaíso, Chile.
- Grillo, E. U., Abbott, K. V., & Lee, T. D. (2010). Effects of masking noise on laryngeal resistance for breathy, normal, and pressed voice. *Journal of Speech, Language, and Hearing Research*, *53*, 850–861.
- Guenther, F. H. (1995). Speech sound acquisition, coarticulation, and rate effects in a neural network model of speech production. *Psychological Review*, *102*, 594–621.
- Gunter, H. E. (2003). A mechanical model of vocal-fold collision with high spatial and temporal resolution. *The Journal of the Acoustical Society of America*, *113*, 994–1000.
- Hillman, R. E., Holmberg, E. B., Perkell, J. S., Walsh, M., & Vaughan, C. (1989). Objective assessment of vocal hyperfunction: An experimental framework and initial results. *Journal of Speech and Hearing Research*, *32*, 373–392.
- Hillman, R. E., Holmberg, E. B., Perkell, J. S., Walsh, M., & Vaughan, C. (1990). Phonatory function associated with hyperfunctionally related vocal fold lesions. *Journal of Voice*, *4*, 52–63.
- Hirano, M., Kurita, S., & Nakashima, T. (1981). The structure of the vocal folds. In K. N. Stevens & M. Hirano (Eds.), *Vocal fold physiology* (pp. 33–41). Tokyo, Japan: University of Tokyo Press.
- Holmberg, E. B., Doyle, P., Perkell, J. S., Hammarberg, B., & Hillman, R. E. (2003). Aerodynamic and acoustic voice measurements of patients with vocal nodules: Variation in baseline and changes across voice therapy. *Journal of Voice*, *17*, 269–282.
- Horáček, J., Šidlof, P., & Švec, J. G. (2005). Numerical simulation of self-oscillations of human vocal folds with Hertz model of impact forces. *Journal of Fluids and Structures*, *20*, 853–869.

- Hsiung, M.-W., & Hsiao, Y.-C.** (2004). The characteristic features of muscle tension dysphonia before and after surgery in benign lesions of the vocal fold. *ORL*, *66*, 246–254.
- Hunter, E. J., Titze, I. R., & Alipour, F.** (2004). A three-dimensional model of vocal fold abduction/adduction. *The Journal of the Acoustical Society of America*, *115*, 1747–1759.
- Ishizaka, K., & Flanagan, J. L.** (1972). Synthesis of voiced sounds from a two-mass model of the vocal cords. *Bell Labs Technical Journal*, *51*, 1233–1268.
- Jiang, J. J., Diaz, C. E., & Hanson, D. G.** (1998). Finite element modeling of vocal fold vibration in normal phonation and hyperfunctional dysphonia: Implications for the pathogenesis of vocal nodules. *Annals of Otolaryngology, Rhinology & Laryngology*, *107*, 603–610.
- Kim, M. J., Hunter, E. J., & Titze, I. R.** (2004). Comparison of human, canine, and ovine laryngeal dimensions. *Annals of Otolaryngology, Rhinology & Laryngology*, *113*, 60–68.
- Kuo, H.-K. J.** (1998). *Voice source modeling and analysis of speakers with vocal-fold nodules* (Unpublished doctoral dissertation). Massachusetts Institute of Technology, Cambridge.
- Liljencrants, J.** (1985). *Speech synthesis with a reflection-type line analog* (Unpublished doctoral dissertation). Royal Institute of Technology, Stockholm, Sweden.
- Lico, A. F., Zañartu, M., González, A. J., Wodicka, G. R., Mehta, D. D., Van Stan, J. H., & Hillman, R. E.** (2015). Real-time estimation of aerodynamic features for ambulatory voice biofeedback. *The Journal of the Acoustical Society of America*, *138*, EL14–EL19.
- Lucero, J. C., & Schoentgen, J.** (2015). Smoothness of an equation for the glottal flow rate versus the glottal area. *The Journal of the Acoustical Society of America*, *137*, 2970–2973.
- Mehta, D., & Hillman, R. E.** (2007). Use of aerodynamic measures in clinical voice assessment. *SIG 3 Perspectives on Voice and Voice Disorders*, *17*(3), 14–18.
- Mehta, D. D., Van Stan, J. H., Zañartu, M., Ghassemi, M., Guttag, J. V., Espinoza, V. M., . . . Hillman, R. E.** (2015). Using ambulatory voice monitoring to investigate common voice disorders: Research update. *Frontiers in Bioengineering and Biotechnology*, *3*, 155.
- Moisik, S. R., & Esling, J. H.** (2014). Modeling the biomechanical influence of epilaryngeal stricture on the vocal folds: A low-dimensional model of vocal-ventricular fold coupling. *Journal of Speech, Language, and Hearing Research*, *57*, S687–S704.
- Morrison, M. D., Nichol, H., & Rammage, L. A.** (1986). Diagnostic criteria in functional dysphonia. *The Laryngoscope*, *96*, 1–8.
- Morrison, M. D., & Rammage, L. A.** (1993). Muscle misuse voice disorders: Description and classification. *Acta Oto-Laryngologica*, *113*, 428–434.
- Murray, P. R., & Thomson, S. L.** (2012). Vibratory responses of synthetic, self-oscillating vocal fold models. *The Journal of the Acoustical Society of America*, *132*, 3428–3438.
- Neils, L. R., & Yairi, E.** (1987). Effects of speaking in noise on vocal fatigue and vocal recovery. *Folia Phoniatrica et Logopaedica*, *39*, 104–112.
- Pelorsson, X., Hirschberg, A., van Hassel, R. R., Wijnands, A. P. J., & Aurégan, Y.** (1994). Theoretical and experimental study of quasisteady-flow separation within the glottis during phonation: Application to a modified two-mass model. *The Journal of the Acoustical Society of America*, *96*, 3416–3431.
- Pemberton, C., Russell, A., Priestley, J., Havas, T., Hooper, J., & Clark, P.** (1993). Characteristics of normal larynges under flexible fiberoptic and stroboscopic examination: An Australian perspective. *Journal of Voice*, *7*, 382–389.
- Perkell, J. S., Hillman, R. E., & Holmberg, E. B.** (1994). Group differences in measures of voice production and revised values of maximum airflow declination rate. *The Journal of the Acoustical Society of America*, *96*, 695–698.
- Regner, M. F., Tao, C., Ying, D., Olszewski, A., Zhang, Y., & Jiang, J. J.** (2012). The effect of vocal fold adduction on the acoustic quality of phonation: *Ex vivo* investigations. *Journal of Voice*, *26*, 698–705.
- Robertson, D., Zañartu, M., & Cook, D.** (2016). Comprehensive, population-based sensitivity analysis of a two-mass vocal fold model. *PLoS One*, *11*(2), e0148309.
- Roy, N., Merrill, R. M., Gray, S. D., & Smith, E. M.** (2005). Voice disorders in the general population: Prevalence, risk factors, and occupational impact. *The Laryngoscope*, *115*, 1988–1995.
- Sama, A., Carding, P. N., Price, S., Kelly, P., & Wilson, J. A.** (2001). The clinical features of functional dysphonia. *The Laryngoscope*, *111*, 458–463.
- Samlan, R. A., & Story, B. H.** (2011). Relation of structural and vibratory kinematics of the vocal folds to two acoustic measures of breathy voice based on computational modeling. *Journal of Speech, Language, and Hearing Research*, *54*, 1267–1283.
- Samlan, R. A., Story, B. H., & Bunton, K.** (2013). Relation of perceived breathiness to laryngeal kinematics and acoustic measures based on computational modeling. *Journal of Speech, Language, and Hearing Research*, *56*, 1209–1223.
- Sapienza, C. M., & Stathopoulos, E. T.** (1994). Respiratory and laryngeal measures of children and women with bilateral vocal fold nodules. *Journal of Speech and Hearing Research*, *37*, 1229–1243.
- Sapienza, C. M., Stathopoulos, E. T., & Brown, W. S., Jr.** (1997). Speech breathing during reading in women with vocal nodules. *Journal of Voice*, *11*, 195–201.
- Scherer, R. C., Alipour, F., Finnegan, E., & Guo, C. G.** (1997). The membranous contact quotient: A new phonatory measure of glottal competence. *Journal of Voice*, *11*, 277–284.
- Södersten, M., & Lindestad, P.-Å.** (1990). Glottal closure and perceived breathiness during phonation in normally speaking subjects. *Journal of Speech and Hearing Research*, *33*, 601–611.
- Sperry, E. E., Hillman, R. E., & Perkell, J. S.** (1994). The use of inductance plethysmography to assess respiratory function in a patient with vocal nodules. *Journal of Medical Speech-Language Pathology*, *2*, 137–145.
- Stager, S. V., Bielamowicz, S. A., Regnell, J. R., Gupta, A., & Barkmeier, J. M.** (2000). Supraglottic activity: Evidence of vocal hyperfunction or laryngeal articulation? *Journal of Speech, Language, and Hearing Research*, *43*, 229–238.
- Stager, S. V., Neubert, R., Miller, S., Regnell, J. R., & Bielamowicz, S. A.** (2003). Incidence of supraglottic activity in males and females: A preliminary report. *Journal of Voice*, *17*, 395–402.
- Stathopoulos, E. T., Huber, J. E., Richardson, K., Kamphaus, J., DeCicco, D., Darling, M., . . . Sussman, J. E.** (2014). Increased vocal intensity due to the Lombard effect in speakers with Parkinson's disease: Simultaneous laryngeal and respiratory strategies. *Journal of Communication Disorders*, *48*, 1–17.
- Stepp, C. E., Hillman, R. E., & Heaton, J. T.** (2010). A virtual trajectory model predicts differences in vocal fold kinematics in individuals with vocal hyperfunction. *The Journal of the Acoustical Society of America*, *127*, 3166–3176.
- Story, B. H.** (1995). *Physiologically-based speech simulation using an enhanced wave-reflection model of the vocal tract* (Unpublished doctoral dissertation). Iowa City: University of Iowa.
- Story, B. H., & Bunton, K.** (2013). Production of child-like vowels with nonlinear interaction of glottal flow and vocal tract resonances. *Proceedings of Meetings on Acoustics*, *19*, 060303.

- Story, B. H., & Titze, I. R.** (1995). Voice simulation with a body-cover model of the vocal folds. *The Journal of the Acoustical Society of America*, *97*, 1249–1260.
- Takemoto, H., Honda, K., Masaki, S., Shimada, Y., & Fujimoto, I.** (2006). Measurement of temporal changes in vocal tract area function from 3D cine-MRI data. *The Journal of the Acoustical Society of America*, *119*, 1037–1049.
- Tao, C., & Jiang, J. J.** (2007). Mechanical stress during phonation in a self-oscillating finite-element vocal fold model. *Journal of Biomechanics*, *40*, 2191–2198.
- Tao, C., Jiang, J. J., & Zhang, Y.** (2006). Simulation of vocal fold impact pressures with a self-oscillating finite-element model. *The Journal of the Acoustical Society of America*, *119*, 3987–3994.
- Thomson, S. L., Mongeau, L., & Frankel, S. H.** (2005). Aerodynamic transfer of energy to the vocal folds. *The Journal of the Acoustical Society of America*, *118*, 1689–1700.
- Titze, I. R.** (1984). Parameterization of the glottal area, glottal flow, and vocal fold contact area. *The Journal of the Acoustical Society of America*, *75*, 570–580.
- Titze, I. R.** (1990). Interpretation of the electroglottographic signal. *Journal of Voice*, *4*, 1–9.
- Titze, I. R.** (2008). Nonlinear source–filter coupling in phonation: Theory. *The Journal of the Acoustical Society of America*, *123*, 2733–2749.
- Titze, I. R.** (2016). Theoretical analysis of maximum flow declination rate versus maximum area declination rate in phonation. *Journal of Speech, Language, and Hearing Research*, *49*, 439–447.
- Titze, I. R., & Alipour, F.** (2006). *The myoelastic aerodynamic theory of phonation*. Iowa City, IA: National Center for Voice and Speech.
- Titze, I. R., & Hunter, E. J.** (2007). A two-dimensional biomechanical model of vocal fold posturing. *The Journal of the Acoustical Society of America*, *121*, 2254–2260.
- Titze, I. R., & Story, B. H.** (2002). Rules for controlling low-dimensional vocal fold models with muscle activation. *The Journal of the Acoustical Society of America*, *112*, 1064–1076.
- Zañartu, M., Galindo, G. E., Erath, B. D., Peterson, S. D., Wodicka, G. R., & Hillman, R. E.** (2014). Modeling the effects of a posterior glottal opening on vocal fold dynamics with implications for vocal hyperfunction. *The Journal of the Acoustical Society of America*, *136*, 3262–3271.
- Zañartu, M., Ho, J. C., Mehta, D. D., Hillman, R. E., & Wodicka, G. R.** (2013). Subglottal impedance-based inverse filtering of voiced sounds using neck surface acceleration. *IEEE Transactions on Audio, Speech, and Language Processing*, *21*, 1929–1939.
- Zañartu, M., Mongeau, L., & Wodicka, G. R.** (2007). Influence of acoustic loading on an effective single mass model of the vocal folds. *The Journal of the Acoustical Society of America*, *121*, 1119–1129.
- Zhang, Y., Tao, C., & Jiang, J. J.** (2006). Parameter estimation of an asymmetric vocal-fold system from glottal area time series using chaos synchronization. *Chaos*, *16*, 023118.
- Zhang, Z.** (2015). Regulation of glottal closure and airflow in a three-dimensional phonation model: Implications for vocal intensity control. *The Journal of the Acoustical Society of America*, *137*, 898–910.

The proposed model is an extension of the (rectangular glottis) body-cover model (BCM) (Story & Titze, 1995). Recent studies have augmented the capabilities of the BCM to investigate the leakage produced by a posterior glottal opening (Zañartu et al., 2014) by allowing for a nonvibratory flow channel connected in parallel to the membranous channel. On the other hand, a two-mass triangular-shaped glottis has been used for speech synthesis (Birkholz et al., 2011a, 2011b), to include the effects of the zipperlike vocal-fold closure commonly observed in female voices (Södersten & Lindestad, 1990).

In this study, a similar solution is used to include prephonatory posturing, allowing for both a posterior and a membranous glottal opening in a single general structure. The proposed model, referred to as the triangular body-cover model (TBCM), relates the rotation and displacement of the arytenoids to the shape of the glottis (see Figure A1), converging to the BCM when no rotation or displacement is present. This approach allows for a low-order approximation of the initial hyperfunctional configuration described by Morrison et al. (1986).

The particular implementation of the flow solution includes the correction made by Lucero and Schoentgen (2015), which avoids some of the numerical issues that the original publication of the BCM produces (Titze, 1984). The TBCM allows for vocal-fold posturing by including both posterior (Zañartu et al., 2014) and membranous glottal gaps (Birkholz et al., 2011a), a refined collision model, and a scheme to link arytenoid posturing to incomplete glottal closure. These additions allow for a more realistic glottal configuration that is critical for studying vocal hyperfunction.

### Equations of Motion

Given that the TBCM is introduced in this article, we briefly describe its mathematical conception. Although only symmetric cases are considered herein, the formulation equally allows for the investigation of asymmetric orientations. Symmetry implies that the displacements of the left masses are equal to those of the right masses (with displacement being measured from the glottal midplane).

The TBCM uses the following equations to describe the vocal-fold dynamics:

$$F_u = m_u \ddot{x}_u = F_{ku} + F_{du} - F_{kc} + F_{eu} + F_{kuCol} + F_{duCol} \quad (A1)$$

$$F_l = m_l \ddot{x}_l = F_{kl} + F_{dl} + F_{kc} + F_{el} + F_{klCol} + F_{dlCol} \quad (A2)$$

$$F_b = m_b \ddot{x}_b = F_{kb} + F_{db} - (F_{ku} + F_{du} + F_{kl} + F_{dl}) - (F_{duCol} + F_{dlCol}), \quad (A3)$$

where  $m$  stands for the mass of each block,  $x$  is the geometric position of each block over time,  $F$  indicates force, the subscript index  $k$  represents spring force,  $d$  represents a damper force,  $e$  is a force produced by the flow pressures,  $c$  stands for the coupling spring between the upper and lower masses, and  $Col$  corresponds to the elements that appear only during collision. The subscript indices  $u$ ,  $l$ , and  $b$  indicate the upper, lower, and body masses, respectively. For modeling purposes, the damper and spring forces were explicitly separated into continuously present components ( $F_{ku}$ ,  $F_{kl}$ ,  $F_{du}$ ,  $F_{dl}$ ) and switched elements that appear only when the masses are colliding ( $F_{kuCol}$ ,  $F_{klCol}$ ,  $F_{duCol}$ ,  $F_{dlCol}$ ).

The definitions of the forces in Equations A1–A3 are similar to the forces originally expressed by Story and Titze (1995), with spring forces of

$$F_{ku} = -k_u \left\{ [(x_u - x_u^0) - (x_b - x_b^0)] + \eta_u [(x_u - x_u^0) - (x_b - x_b^0)]^3 \right\} \quad (A4)$$

$$F_{kl} = -k_l \left\{ [(x_l - x_l^0) - (x_b - x_b^0)] + \eta_l [(x_l - x_l^0) - (x_b - x_b^0)]^3 \right\} \quad (A5)$$

$$F_{kb} = -k_b \left[ (x_b - x_b^0) + \eta_b (x_b - x_b^0)^3 \right] \quad (A6)$$

$$F_{kc} = -k_c [(x_l - x_l^0) - (x_u - x_u^0)], \quad (A7)$$

where  $k$ s are linear spring constants,  $\eta$ s are nonlinear spring constants, and  $x^0$ s are the rest positions of the respective masses. For all these parameters, a set of controlling rules are used to assign a determinate value (Titze & Story, 2002). In a similar manner, the damping forces are

$$F_{du} = -2\zeta_u \sqrt{m_u k_u} (\dot{x}_u - \dot{x}_b) \quad (\text{A8})$$

$$F_{dl} = -2\zeta_l \sqrt{m_l k_l} (\dot{x}_l - \dot{x}_b) \quad (\text{A9})$$

$$F_{db} = -2\zeta_b \sqrt{m_b k_b} (\dot{x}_b), \quad (\text{A10})$$

where  $\zeta_u$ ,  $\zeta_l$ , and  $\zeta_b$  are the damping ratios of the noncolliding upper, lower, and body masses, respectively.

When the masses are colliding (e.g., the displacement of one mass is overlapping the opposing mass), the collision of the triangular shape is proportional to the slope of the anterior–posterior border. Therefore, the resulting vocal-fold collision is progressive and can be considered as the integration of collision forces across the length of the glottis:

$$F_{kuCol} = \int_{L_{uClosed}} F_{kuCol}(z) dz \quad (\text{A11})$$

$$F_{klCol} = \int_{L_{lClosed}} F_{klCol}(z) dz, \quad (\text{A12})$$

where, following Story and Titze (1995), for each point on the z-axis we have

$$F_{kuCol}(z) = -\tilde{k}_{uCol} \left[ (x_u(z) - x_u^{Col}) + \tilde{\eta}_{uCol} (x_u(z) - x_u^{Col})^3 \right] \quad (\text{A13})$$

$$F_{klCol}(z) = -\tilde{k}_{lCol} \left[ (x_l(z) - x_l^{Col}) + \tilde{\eta}_{lCol} (x_l(z) - x_l^{Col})^3 \right] \quad (\text{A14})$$

for the symmetric case. The collision points  $x_u^{Col}$  and  $x_l^{Col}$  for the upper and lower masses occur on the midplane; therefore, Equations A13 and A14 become

$$F_{kuCol}(z) = -\tilde{k}_{uCol} (x_u(z) + \tilde{\eta}_{uCol} x_u^3(z)) \quad (\text{A15})$$

$$F_{klCol}(z) = -\tilde{k}_{lCol} (x_l(z) + \tilde{\eta}_{lCol} x_l^3(z)), \quad (\text{A16})$$

where  $\tilde{k}_{uCol}$  and  $\tilde{k}_{lCol}$  are the linear collision spring constants and  $\tilde{\eta}_{uCol}$  and  $\tilde{\eta}_{lCol}$  are the nonlinear collision spring constants across the length of the glottis. For simplicity, these values are considered constants on the z-axis, meaning that the collision spring does not vary in the anterior–posterior direction.

The slope of the displacement of the borders in the anterior–posterior direction is given by

$$x_u(z) = x_u + \frac{\Delta x_u}{L_g} z \quad (\text{A17})$$

$$x_l(z) = x_l + \frac{\Delta x_l}{L_g} z, \quad (\text{A18})$$

where  $\Delta x_u$  and  $\Delta x_l$  are the prephonatory posterior glottal distance produced in the posterior border relative to the anterior border as a consequence of prephonatory posturing. The symbol  $L_g$  is defined as the vibratory length of the glottis, and is obtained from muscle-activation rules (Titze & Story, 2002). Because the arytenoid cartilages have a pyramidal shape, the prephonatory displacement of the posterior border may eventually be different for the upper and lower masses. However, in this article the posterior glottal distance is considered symmetric about the upper and lower masses. Note that we maintained the original rules of muscle activation (Titze & Story, 2002) that relate physiological configurations with underlying model parameters in our design of the TBCM and created separate rules for controlling the arytenoid rotation.

The total spring collision force can then be defined as

$$F_{kuCol} = -\tilde{k}_{uCol} L_g \alpha_u [(x_u + 0.5\Delta x_u \alpha_u) + \tilde{\eta}_{uCol} (x_u^3 + 1.5x_u^2 \Delta x_u \alpha_u + x_u \Delta x_u^2 + \alpha_u^2 + 0.25\Delta x_u^3 \alpha_u^3)] \quad (A19)$$

$$F_{klCol} = -\tilde{k}_{lCol} L_g \alpha_l [(x_l + 0.5\Delta x_l \alpha_l) + \tilde{\eta}_{lCol} (x_l^3 + 1.5x_l^2 \Delta x_l \alpha_l + x_l \Delta x_l^2 + \alpha_l^2 + 0.25\Delta x_l^3 \alpha_l^3)], \quad (A20)$$

where  $\alpha = L_{closed}/L_g$  is a proportionality factor that indicates how much surface of the mass is actually colliding (also called the *membranous contact quotient* by Scherer et al., 1997). If  $\tilde{k}_{Col} = h_{Col}/L_g$  and  $\tilde{\eta}_{Col} = \eta$ , this formulation of collision spring force converges to the BCM equation as  $\Delta x \rightarrow 0$ , since in the limit case the value of  $\alpha$  can only switch between 0 and 1. In addition, this solution is an extension of the work presented by Birkholz et al. (2011b), wherein linear springs ( $\eta = 0$ ) are used in an oblique collision simulation.

Damping forces are separated into two elements: normal (Equations A8–A10) and collision (Equations A21 and A22). The latter will be affected by the oblique configuration, since in the TBCM the mass is progressively colliding. The damping collision forces are defined as

$$F_{duCol} = -2\zeta_{uCol} \alpha_u \sqrt{m_u k_u} (\dot{x}_u - \dot{x}_b) \quad (A21)$$

$$F_{dlCol} = -2\zeta_{lCol} \alpha_l \sqrt{m_l k_l} (\dot{x}_l - \dot{x}_b), \quad (A22)$$

where  $\zeta_{uCol}$  and  $\zeta_{lCol}$  are the damping coefficients of collision for the upper and lower masses, respectively, with a value of 0.4 set herein according to Story and Titze (1995).

Assuming a linear positive displacement of the posterior border in relation to the anterior border of the glottis, with a symmetric case a new glottal area is produced:

$$A_u = (1 - \alpha_u) L_g (x_u + \Delta x_u) \quad (A23)$$

$$A_l = (1 - \alpha_l) L_g (x_l + \Delta x_l). \quad (A24)$$

To solve for the intraglottal pressures, we used an approach of consecutive infinitesimal independent flow channels, where it was assumed that the pressures are the same as in the BCM (Story & Titze, 1995). That is,

$$P_u = \begin{cases} 0; & A_u = 0 \\ P_i; & A_u > 0 \end{cases} \quad (A25)$$

$$P_u = \begin{cases} 0; & A_l = 0 \\ P_s - (P_s - P_i) \left(\frac{A_{min}}{A_l}\right)^2; & A_l > 0, \end{cases} \quad (A26)$$

where  $P_s$  and  $P_i$  are the subglottal and supraglottal pressures, respectively, in the borders of the glottal system with the vocal tract, and  $A_{min}$  represents the minimum area between the upper and lower masses. The extension of Equations A25 and A26

for consecutive infinitesimal independent channels can be expressed as  $P_u(z)$  and  $P_l(z)$ ; therefore, the total force applied to each mass is

$$F_{eu} = T_u \int_{L_g} P_u(z) dz \quad (A27)$$

$$F_{el} = T_l \int_{L_g} P_l(z) dz, \quad (A28)$$

where  $T_u$  and  $T_l$  are the thickness of the upper and lower layers of the cover, respectively. It can be shown that for a glottal shape defined by Equations A17 and A18, the total force applied to each mass is

$$F_{eu} = T_u P_i (1 - \alpha_u) L_g \quad (A29)$$

$$F_{el} = T_l \left[ P_s (1 - \alpha_l) L_g - (P_s - P_i) \left( L_D + \int_{L_C} \frac{x_u^2(z)}{x_l^2(z)} dz \right) \right], \quad (A30)$$

where  $L_D$  and  $L_C$  are the portions of the glottis where the displacements of the upper and lower masses produce a divergent or a convergent channel, respectively.

### Incomplete Glottal Closure

In the proposed model, the arytenoids move in the transverse plane with two degrees of freedom: rotation ( $a_r^\circ$ ) and displacement ( $a_r^d$ ). Zero rotation and zero displacement means a fully closed glottis. A positive rotation is defined as causing separation of the arytenoids at the vocal process. Positive displacement of the arytenoids is defined as the distance of the base of the cartilaginous glottis (see Figure A2). The resulting shape of the glottis with the arytenoid rotation and displacement is triangular (Birkholz et al., 2011a; Samlan & Story, 2011). In this configuration,  $L_a$  is the arytenoid face.

The posterior glottal distance, using the configuration previously defined, is obtained by

$$PGD = 2(a_r^d + L_a \sin(a_r^\circ)). \quad (A31)$$

Therefore, the posterior and membranous glottal openings, for positive rotation and arytenoid displacements, can be calculated as

$$PGO = \gamma L_a \cos(a_r^\circ) (PGD - \gamma L_a \sin(a_r^\circ)) \quad (A32)$$

$$MGO = \frac{1}{2} L_g PGD, \quad (A33)$$

where  $\gamma$  is the open portion of the arytenoid cartilage that interacts with the flow channel.

Incomplete closure has also been described in terms of a *glottal angle* (Cooke et al., 1997; Dailey et al., 2005; Hunter et al., 2004; Stepp et al., 2010), which is measured between glottal edges at the anterior commissure (see Figure A2). Therefore, the conversion from a symmetric arytenoid rotation to glottal angle is given by

$$\text{glottal angle} = 2 \tan^{-1} (PGD/L_g). \quad (A34)$$

Figure A1. Triangular body-cover model. PGO = posterior glottal opening.

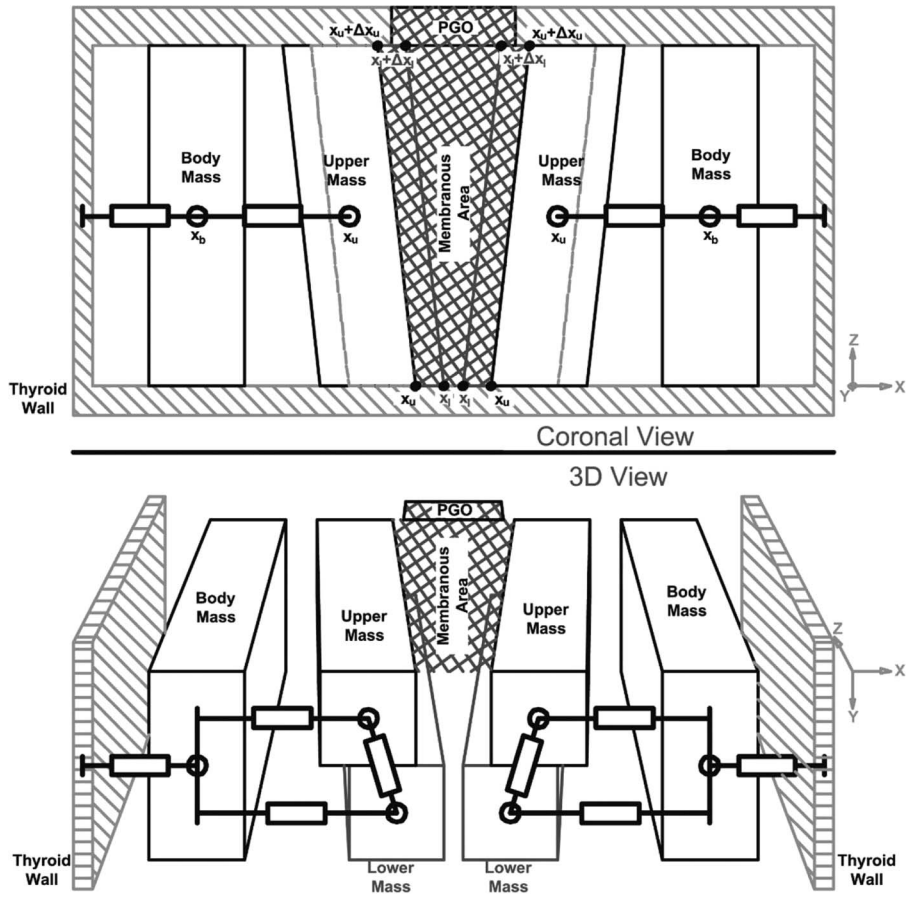


**Figure A2.** Arytenoid posturing and its equivalent on the proposed model. PGO = posterior glottal opening; MGO = membranous glottal opening; PGD = posterior glottal displacement;  $a_r^d$  = arytenoid displacement;  $a_r^o$  = arytenoid rotation;  $L_a$  = arytenoid face.

